AD-A257 928

JMENTATION PAGE

Form Approved
OBM No. 0704-0188

.. Agency Use Only (Leave blank).	2. Report Date. March 1992	3. Report Type and Dates Covered. Final - Proceedings

4. Title and Subtitle.
Radiation and Scattering at Oblique Incidence from Submerged Oblong Elastic Bodies

5. Funding Numbers.

Contract	
Program Element No.	0601153N
Project No.	03202
Task No.	340
Accession No.	DN255011
Work Unit No.	12212B

6. Author(s).
Herbert Uberall*, X. L. Bao*, Russel D. Miller**, and Michael F. Werby

7. Performing Organization Name(s) and Address(es).
Naval Oceanographic and Atmospheric Research Laboratory
Ocean Science Directorate
Stennis Space Center, MS 39529-5004

8. Performing Organization Report Number.
PR 92:105:221

9. Sponsoring/Monitoring Agency Name(s) and Address(es).
Naval Oceanographic and Atmospheric Research Laboratory
Ocean Acoustics and Technology Directorate
Stennis Space Center, MS 39529-5004

10. Sponsoring/Monitoring Agency Report Number.
PR 92:105:221

11. Supplementary Notes.
Pulished in Second International Congress on Recent Developments in Air- and Structure-Borne Sound and Vibration
*Department of Physics, Catholic University of America, Washington, DC 20064
**NKF Engineering, Arlington, VA 22203-1800

12a. Distribution/Availability Statement.
Approved for public release; distribution is unlimited.

12b. Distribution Code.

13. Abstract *(Maximum 200 words).*

The resonant behavior of solid or hollow oblong submersed elastic objects is studied both theoretically and experimentally. The resonances have been studied directly, by a calculation of surface wave displacements, or inferentially, by calculations or observations of echoes from plane incident acoustic waves with axial, broadside, or general oblique incidence onto the submersed objects. For the latter, we considered solid or hollow spheroids, or cylinders with flat or with hemispherical ends. Resonances are obtained theoretically from the phase matching of surface waves, which physically form standing waves in this case. A bar wave picture of resonant vibration has also been considered; it is shown to apply in the low-ka region while surface wave pictures apply in the high-ka region while surface wave pictures apply in the high-ka region, and the two pictures merge in the intermediate region. The dispersion of surface waves along the object for axial incidence is treated exactly. For broadside incidence, simultaneous excitation of meridional and circumferential surface wave is noted. The same surface wave picture applies for sound radiation from these objects following point excitation.

14. Subject Terms.
Acoustic scattering, shallow waer, waveguide propagation

15. Number of Pages.
8

16. Price Code.

17. Security Classification of Report.	18. Security Classification of This Page.	19. Security Classification of Abstract.	20. Limitation of Abstract.
Unclassified	Unclassified	Unclassified	SAR

PROCEEDINGS

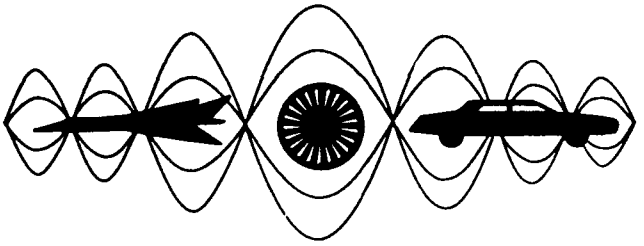

SECOND INTERNATIONAL CONGRESS ON RECENT DEVELOPMENTS IN AIR- AND STRUCTURE-BORNE SOUND AND VIBRATION

MARCH 4-6, 1992 AUBURN UNIVERSITY, USA

Edited by

Malcolm J. Crocker

P. K. Raju

Volume 3

SECOND INTERNATIONAL CONGRESS ON
RECENT DEVELOPMENTS IN AIR- AND
STRUCTURE-BORNE SOUND AND VIBRATION
MARCH 4-6, 1992 AUBURN UNIVERSITY, USA

RADIATION AND SCATTERING AT OBLIQUE INCIDENCE FROM SUBMERGED OBLONG ELASTIC BODIES

Herbert Überall and X. L. Bao
Department of Physics
Catholic University of America, Washington, DC 20064, USA

Russel D. Miller
NKF Engineering
Arlington, VA 22203-1800, USA

Michael F. Werby
NRL, Numerical Modeling Branch
Stennis Space Center, MS 39529-5000, USA

ABSTRACT

The resonant behavior of solid or hollow oblong submersed elastic objects is studied both theoretically and experimentally. The resonances have been studied directly, by a calculation of surface wave displacements, or inferentially, by calculations or observations of echoes from plane incident acoustic waves with axial, broadside, or general oblique incidence onto the submersed objects. For the latter, we considered solid or hollow spheroids, or cylinders with flat or with hemispherical ends. Resonances are obtained theoretically from the phase matching of surface waves, which physically form standing waves in this case. A bar wave picture of resonant vibration has also been considered; it is shown to apply in the low-ka region while surface wave pictures apply in the high-ka region, and the two pictures merge in the intermediate region. The dispersion of surface waves along the object for axial incidence is treated exactly. For broadside incidence, simultaneous excitation of meridional and circumferential surface wave is noted. The same surface wave picture applies for sound radiation from these objects following point excitation.

INTRODUCTION

Experimental studies on the resonant behavior of submersed elastic objects, subject to incident acoustic waves and pulses, have been carried out for about a decade at US [1-3], German [4], and especially at French acoustics laboratories [5-8]. These studies were motivated by the establishment of the acoustic Resonance Scattering Theory (RST) [9-11] which, together with the physical interpretation of the elastic-body resonances in terms of phase-matching surface waves [12], has been brilliantly verified by the experiments. The outcome of these studies, of which the above references [1-8] just constitute a small, representative selection (for more recent updates on the extensive investigations that have been performed on this subject, see the books quoted in Refs. [3] and [11]) consists in the following information:

(a) The eigenfrequencies of elastic objects were determined from the observed resonance spectra. This was done first for the simplest objects such as solid spheres and infinite (i.e.) very long cylinders, but subsequently also for solid and hollow objects of more complex shapes, mainly for spheroids and finite cylinders with flat or hemispherical endcaps. This also includes the strength of the acoustic excitation (i.e., the peak heights), and the widths of the resonance peaks.

(b) Using phase matching arguments, the observed resonances were classified in terms of the surface waves that generated them (a surface wave launched by the incident wave, which is circumnavigating the object on a closed path, causes a resonant buildup of the surface wave amplitude, and hence resonant scattering, if phase matching takes place upon each circumnavigation). This led immediately to a classification of the various kinds of surface waves that the submersed elastic object can support, and that were in fact excited by the incident wave.

(c) The spacing of the resonance families belonging to a given type of surface waves permitted a prediction of the dispersion curves of each of these surface wave types; both phase and group velocities, and the losses due to radiation could be obtained in this way.

(d) A convenient way of representing the above data consists in plotting the "Regge trajectories" of each surface wave type, where the successive mode numbers in each wave are graphed vs. the frequency values at which the mode resonates.

In addition to such studies of the surface waves on elastic objects, excited by incident acoustic waves and inferred from the resonances they generate as observed in scattered echoes, the surface waves have also been examined when generated by mechanical forces acting on the elastic object, leading to acoustic radiation that displays related resonance effects [13]. Both scattering and radiation-generated resonances will be discussed in the following.

SURFACE WAVE GENERATION: BROADSIDE VS. END-ON

It was shown for cylinder and sphere scattering that analytically, resonances in the scattering amplitude are described [9, 10] by terms of the form

$$1/(x_{n\ell} - x - i\Gamma_{n\ell}/2) \qquad (1)$$

where $x = ka$, k being the wave number in the ambient fluid and a the cylinder or sphere radius. For oblong bodies, e.g. spheroids, one may instead use the variable $X = kL/2$, L being the length of the object. Equation (1) shows that the resonant amplitude has poles in the complex frequency plane located at

$$x = x_{n\ell} - i\Gamma_{n\ell}/2, \qquad (2)$$

i.e. in the fourth quadrant. For electromagnetic waves, this has been noted by Baum [14], who based his "Singularity Expansion Method (SEM)" of electromagnetic scattering on this concept. On the other hand, it was shown by Franz [15] by applying the Watson transformation to the modal series of scattering, that circumferential ("creeping" or "surface") waves arise in the scattering process, which e.g. for a cylinder have the

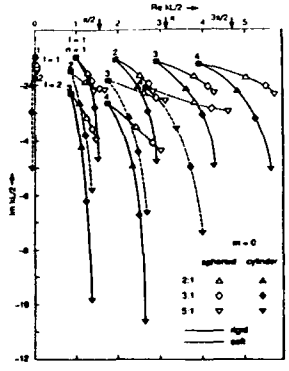

Fig. 1. Complex eigenfrequencies of rigid and soft elongated bodies.

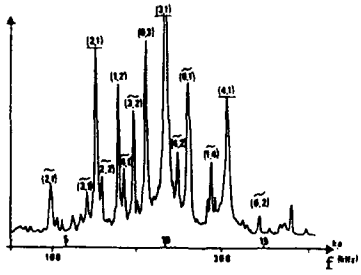

Fig. 2. Resonances of WC cylinder (experimental, broadside incidence).

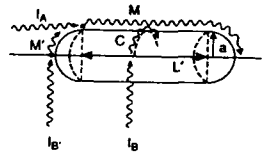

Fig. 3. Generation of circumferential and meridional surface waves by broadside incidence on a hemispherically-capped cylinder.

form $\exp(i\nu\phi)$, with a circumferential propagation constant ν given by $\nu = \nu_\ell$, which are the location of poles of the scattering amplitude in the complex ν-plane obtained from the Watson transformation; these are known as the "Watson poles" in electromagnetics, or "Regge poles" in nuclear physics. The connection between SEM poles and Watson-Regge poles was established by Dickey and Überall [16] in 1978.

The ℓth surface wave $\exp(i\nu_\ell\phi)$ becomes resonant at $\nu_\ell = n$ because then, an integer number of wavelengths fits the circumference of the scatterer. This "principle of phase matching" [12,17] can be used to determine the nth modal resonance frequency (i.e., the position of the corresponding SEM pole) from the resonance condition

$$\nu_\ell = n. \tag{3}$$

This leads to the physical picture of the resonances, showing that a resonance originates from the resonant buildup of a multiply circumnavigating surface wave when it matches phase after each encirclement of the scatterer. This principle can be used in order to determine the resonance frequencies of bodies of arbitrary shape [17], the task here is mainly to obtain the surface paths of resonating surface waves. As an example of this approach, we show in Fig. 1 the complex resonance frequencies $X_{n\ell} = (L/2a)x_{n\ell}$ obtained by the phase matching condition for rigid or soft spheroids and hemispherically-endcapped cylinders of length L and radius a, for aspect ratios 2:1, 3:1, and 5:1 and assuming meridionally propagating surface waves, i.e., axial incidence of the acoustic wave generating these surface waves [18].

The results of an experimental study on the resonances of a solid tungsten carbide cylinder of finite length, terminated by hemispherical endcaps, are in press [8]. Both axial and broadside incidence was employed here. The interesting features appearing in Fig. 2 which shows the backscattering spectrum at broadside incidence, are the fact that not only the resonances that correspond to the phase matching of surface waves propagating circumferentially around the cylinder are visible [labeled by (n,ℓ) where n = mode number, ℓ = 1, 2, 3 surface-wave family index], but also those of meridionally propagating surface waves, labeled by $(n,\tilde{\ell})$. All the latter resonances are those, and only those, seen in the backscattering spectrum for axial incidence in the same experiment [8]. The reason for the broadside excitation of both types of closed-path surface wave phase-match resonances is schematically shown in Fig. 3 (although this figure refers to an impenetrable cylinder, hence tangential excitation of the surface waves): the meridional wave gets excited on the endcaps.

Graphs analogous to Fig. 2, obtained from a T-matrix calculation of backscattering for axial and broadside incidence for a 4:1 nickel spheroid, are shown e.g. in Ref. [19], reproduced below in Fig. 4, (a) for axial and (b) for broadside incidence. The form function (a) shows the n = 2 Rayleigh-wave peak at kL/2 = 7.0, caused by the phase matching of a meridionally propagating Rayleigh wave. The same peak also appears at broadside incidence (b), indicating that even in this case, meridional waves were

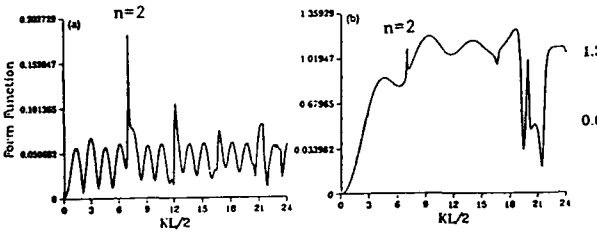

Fig. 4. Residual response vs. kL/2 for a 4:1 nickel spheroid: (a) end-on incidence, (b) broadside incidence.

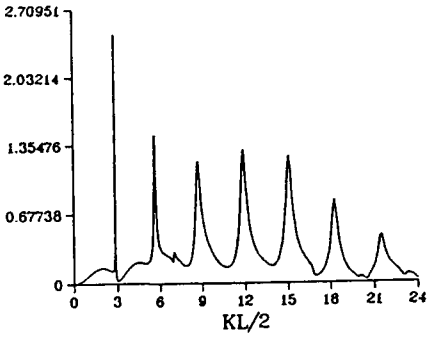

Fig. 6. As in Fig. 4, incidence at 50° to symmetry axis.

generated (while generally, the surface waves generated here propagate equatorially around the object, see Fig. 3).

In Fig. 4a, the first resonance frequency is lower than in the broadside case of Fig. 4b. This is because in broadside incidence, the surface waves follow a minimal path around the spheroid, i.e., parallel to the equator. For end-on incidence, the surface waves follow a maximal path, i.e. around a meridian. Thus the resonance frequency is higher for broadside incidence.

SURFACE WAVES FROM OBLIQUE INCIDENCE

Experiments on the excitation of surface waves on elastic cylinders and cylindrical shells by obliquely incident waves have been carried out at French laboratories since 1986 [20,21]. The important discovery here was the observation of resonances caused by axially propagating waves ("guided waves"), analogous to the above-mentioned meridional waves. The combination of circumferential and guided waves can be viewed as leading to helically propagating waves [22,23]. An example for these is given in Fig. 5, where the simplest closed geodesics ("helicoidal paths") for spheroids are shown; these paths were used to predict by phase matching the electromagnetic resonance frequencies of conducting spheroids [24].

In the elastic-body case, Fig. 6 shows resonances excited by oblique acoustic incidence, at 50° to the symmetry axis, in the nickel spheroid mentioned above. Here, bending resonances are dominant in which the spheroid (at 4:1 being sufficiently long and bar-like) undergoes bending vibrations about its long axis; and these are strongly excited by obliquely incident waves.

The question has been brought up [25] whether the resonances generated by axially incident signals can also be interpreted in terms of (longitudinal) bar waves. In the surface wave picture, the resonances are determined by the phase matching condition.

$$\oint k_\ell \, ds = 2\pi (n + \tfrac{1}{2}), \quad n = 1,2,3... \tag{4}$$

integrated over a closed surface path, while bar waves require

$$2 \int_0^L k_\ell{}^b \, dx = 2\pi m, \qquad m = 1,2,3..., \tag{5}$$

k_ℓ and $k_\ell{}^b$ being the wave numbers of the corresponding waves and m the number of half-wavelengths along the overall length L of the object. For $k_\ell{}^b$, we use the wave number for an infinite cylinder, while for k_ℓ in Eq. (4) one can employ the "tangent sphere" approximation where e.g. on a spheroid, the surface wave path is locally approximated by that on a tangent sphere [17], with known values of k_ℓ. In that method, a constant (Rayleigh-type) wave number can be employed on the cylindrical portion of e.g. a cylinder with hemispherical endcaps. This will be referred to as PM-TS. However, the known wave number on an infinite solid cylinder can be used for this purpose (an example being shown in Fig. 7 for a steel cylinder, the phase velocity tending to that of the Rayleigh were at high frequencies), thereby taking the transverse curvature into account. This model will be called PM-IC. Using the dispersion curve of Fig. 7, one may also employ the "bar wave" resonance condition Eq. (5); that model can be called LBW. We have applied all these models [26] to hemispherically capped steel cylinders as shown in Fig. 8. Here, the Regge trajectories indicate, by comparison with experimental results shown as circles, the correctness of phase matching (PM-IC and PM-TS) at high frequencies. Low frequency experiments are not available in this case, but for other examples these showed that both the bar wave and especially the PM-IC

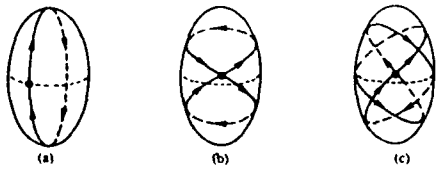

Fig. 5. Examples of simple closed geodesics on a prolate spheroid.

model fit the data well at low frequencies.

RADIATION PROBLEMS

We next consider the radiation and scattering from a stiffened cylindrical shell with flat flexible endcaps [27]. The NASTRAN/SIERRAS code was used to perform mobility, radiation and scattering analysis for the shell. The NASTRAN program is a general purpose finite element code. In the NASTRAN/SIERRAS approach it is used to obtain the structural matrices used by SIERRAS to represent the dynamic response of the structure in vacuo. The SIERRAS (Surface Integral Equation Radiation and Scattering) code is an advanced boundary element code for analyzing the radiation and scattering from arbitrary structures [28,29].

The NASTRAN finite element model consists of approximately 10000 degrees of freedom (DOF). It includes four plate elements between stiffeners and grid points every five degrees around the circumference. Guyan reduction was used to reduce the analysis set to 813 DOF prior to running SIERRAS. The analysis set included one grid point between stiffeners and a point every ten degrees around the circumference.

The SIERRAS boundary element model uses 437 wet fluid degrees of freedom in the analysis. The fluid element is a nine-noded superparametric boundary element.

The measured and computed radial drive point mobility is shown in Figure 9. The forced point was on the center stiffener at the midpoint of the shell in the radial direction. The peaks shown on the figure are the (1,2), (1,3), (1,1), and (1,4) modes of the shell, respectively. The mode numbers refer to the number of longitudinal half waves and the number of circumferential whole waves. Therefore the 1,4 wave consists of one longitudinal half wave along the shell and four whole waves around the circumference.

The radiated noise from the shell is given in Figure 10. Measured and computed results are shown for a location 60 feet in the radial direction from the drive point. The (1,1) mode is responsible for the wide peak at 300 Hz and corresponds to the bending mode of the cylinder.

Finally, the scattering for the shell for broadside incidence is shown in Figure 11. Although no measured results are provided, the comparisons with radiated noise measurements above and previous scattering analyses [28,29] yield a reasonable level of confidence in the results. The scattering results are normalized by a factor of R/a where R is the distance of the observation point and a is the radius of the cylinder. Note that while the frequencies of the resonances are comparable, the magnitudes or response are different. The maximum radiated noise was obtained for the (1,2) mode

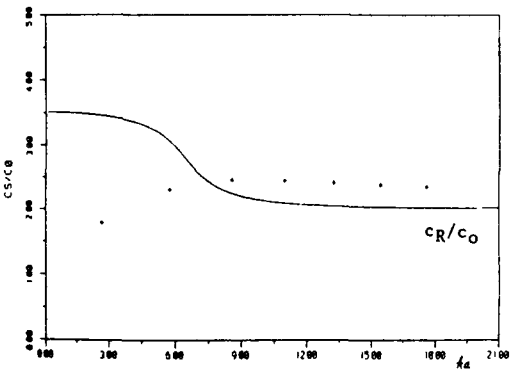

Fig. 7. Dispersion curves of the lowest axisymmetrical mode for an infinite steel cylinder (curve) and a steel sphere (crosses).

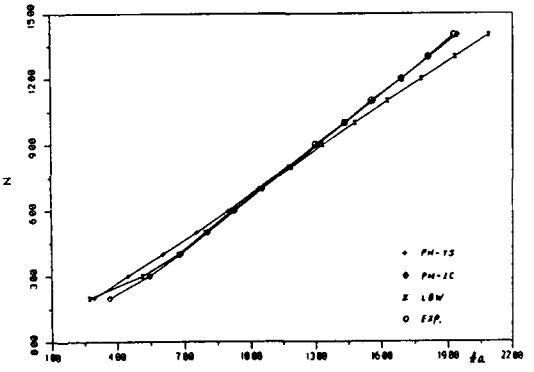

Fig. 8. Regge trajectory (number of resonating mode vs. frequency) for solid steel cylinde with hemispherical endcaps, aspect ratio = 2, end-on incidence.

while the maximum scattering was found for the (1,1) bending mode. Scattered pressure favors the lowest modes of the shell. The reason for this difference lies in the fact that the incident plane wave will tend to excite the resonance in a more pure form than a point force. Therefore, below coincidence, the cancellation of lobes over the surface is more likely to occur with scattering than for point excitation.

REFERENCES

[1] S. K. Numrich, W. E. Howell, J. V. Subrahmanyam, and H. Überall, "Acoustic ringing response of the individual resonances of an elastic cylinder," J. Acoust. Soc. Am. 80 (1986) 1161-1169.

[2] S. G. Kargl and P. L. Marston, "Observations and modeling of the backscattering of short tone bursts from a spherical shell: Lamb wave echoes, glory, and axial reverberations," J. Acoust. Soc. Am. 85 (1989) 1014-1028.

[3] X. L. Bao, H. Überall, and J. Niemiec, ""Experiments on the excitation of resonances of elastic objects by acoustic pulses, and theoretical interpretation," in Mechanics Pan-America, special issue of Applied Mechanics Reviews, 1991 (in press); X. L. Bao and H. Überall, "Experimental study of acoustic resonances of elastic spheres and hemispherically endcapped cylinders," in Acoustic Resonance Scattering, H. Überall, ed., Gordon and Breach, New York, 1992 (in press).

[4] H. Peine, Diplomarbeit, III. Physikalisches Institut, Universität Göttingen, Germany (1988).

[5] G. Maze and J. Ripoche, "Méthode d'isolement et d'identification des résonances (MIIR) de cylindres et de tubes soumis à une onde acoustique plane dans l'eau," Rev. Phys. Appl. 18 (1983) 319-326.

[6] M. Talmant and G. Quentin, "Backscattering of a short ultrasonic pulse from thin cylindrical shells," J. Appl. Phys. 63 (1988) 1857-1863.

[7] M. Talmant, G. Quentin, J. L. Rousselot, J. V. Subrahmanyam, and H. Überall, "Acoustic resonances of thin cylindrical shells and the resonance scattering theory," J. Acoust. Soc. Am. 84 (1988) 681-688.

[8] G. Maze, F. Lecroq, D. Decultot, J. Ripoche, S. K. Numrich, and H. Überall, "Acoustic scattering from finite cylindrical elastic objects," J. Acoust. Soc. Am., in press.

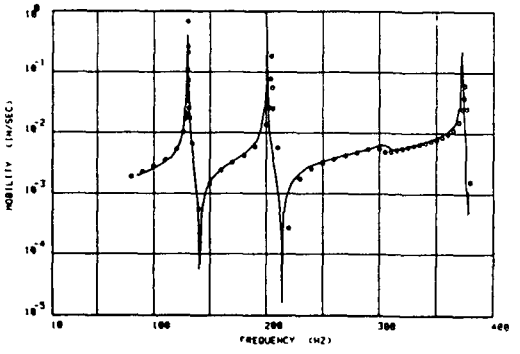

Fig. 9. Drive point mobility of a stiffened cylindrical shell (curve: measured; circles: NASTRAN/SIERRAS theoretical results).

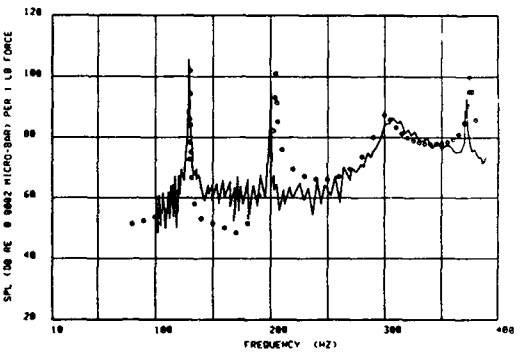

Fig. 10. Radiated noise of a force-excited stiffened cylindrical shell at a radial distance of 60' from drive point (curve: measured; circles: NASTRAN/SIERRAS).

[9] H. Überall, "Modal and surface-wave resonances in acoustic-wave scattering from elastic objects and in elastic-wave scattering from cavities, in Int. Union Theoret. and Applied Mech. (IUTAM) Symposium: Modern Problems in Elastic Wave Propagation, edited by J. Miklowitz and J. Achenbach, Northwestern Univ., Sept. 1977; Proceedings publ. by Wiley (1978) 239-263.

[10] L. Flax, L. R. Dragonette, and H. Überall, "Theory of elastic resonance excitation by sound scattering," J. Acoust. Soc. Am. 63 (1978) 723-731.

[11] A. Derem, "Théorie de la matrice S et transformation de Sommerfeld-Watson dans la diffusion acoustique," in N. CESPA, La Diffusion Acoustique, edited by B. Poiree, CEDOCAR, Paris (1987) 189-279.

[12] H. Überall, L. R. Dragonette, and L. Flax, "Relation between creeping waves and normal modes of vibration of a curved body," J. Acoust. Soc. Am. 61 (1977) 711-715.

[13] P. Pareige, "Spectroscopie des résonances acoustiques," Thesis, University of Le Havre, 1988.

[14] C. E. Baum, in Transient Electromagnetic Fields, L. B. Felsen, ed., Springer, Berlin/Heidelberg 1976, 129-179.

[15] W. Franz, Über die Greenschen Funktionen des Zylinders und der Kugel," Zeits. f. Naturforsch. 9a (1954) 705-716.

[16] J. W. Dickey and H. Überall, "Surface wave resonances in sound scattering from elastic cylinders," J. Acoust. Soc. Am. 63 (1978) 319-320.

[17] H. Überall, Y. J. Stoyanov, et al., "Resonance spectra of elongated elastic objects," J. Acoust. Soc. Am. 81 (1987) 312-316.

[18] X. L. Bao, C. R. Schumacher, and H. Überall, "Complex resonance frequencies in acoustic wave scattering from impenetrable spheres and elongated objects," J. Acoust. Soc. Am. 90 (1991) 2118-2123.

[19] M. F. Werby et al., "Sound scattering from submerged elastic objects and shells of general shape," Proc. 3rd IMACS Symposium on Computational Acoustics, Harvard University, Cambridge, MA, June 1990.

[20] J. L. Izbicki, "Diffusion acoustique par des cylindres et des tubes," Thesis, University of Le Havre, 1986.

[21] P. Rembert, O. Lenoir, F. Lecroq, and J. L. Izbicki, "Oblique scattering by cylindrical shells," Phys. Lett. A157 (1991) 495-502.

[22] H. Überall et al., "Complex acoustic and electromagnetic resonance frequencies of prolate spheroids and related elongated objects and their physical interpretation," J. Appl. Phys. 58 (1985) 2109-2124.

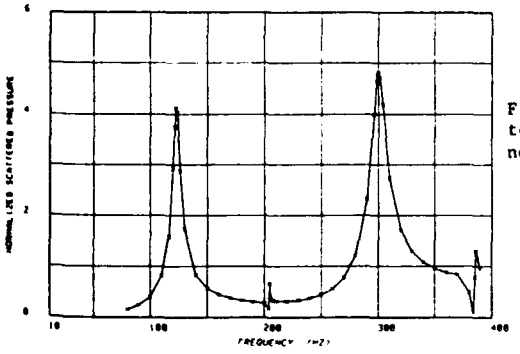

Fig. 11. Normalized form function (backscattering) for a stiffened cylindrical shell at normal distance (NASTRAN/SIERRAS results).

[23] J. M. Conoir, "Resonance scattering theory for oblique incidence," in Electromagnetic and Elastic Scattering, World Scientific, Singapore (1988).

[24] B. L. Merchant, A. Nagl, and H. Überall, "Eigenfrequencies of conducting spheroids and their relation to helicoidal surface wave paths," IEEE Trans. Antennas Propagat. 37 (1989) 629-634.

[25] R. Hackman, G. Sammelmann, K. Williams , and D. Trivett, "A reanalysis of the acoustic scattering from elastic spheroids," J. Acoust. Soc. Am. 83 (1988) 1255-1266.

[26] X. L. Bao, H. Überall and J. Niemiec, "Sound scattering and resonance prediction for a finite elastic cylinder immersed in water," J. Acoust. Soc. Am. (to be published).

[27] L. H. Chen, "Acoustic emission from submerged structures," Developments in Boundary Element Methods 2, edited by P. K. Banerjee and R. P. Show, Applied Science Publishers, Ltd., England, 1982.

[28] R. D. Miller, H. Huang, E. T. Moyer, and H. Überall, "The analysis of the radiated and scattered acoustic fields from submerged shell structures using a modal finite element/boundary element formulation," in Numerical Techniques in Acoustic Radiation (American Society of Mechanical Engineers, New York, NCA vol. 6 (1989), 83-94.

[29] R. D. Miller, E. T. Moyer, and H. Überall, "A comparison between the boundary element method and the wave superposition approach for the analysis of the scattered fields from rigid bodies and elastic shells," J. Acoust. Soc. Am. 89 (1991) 2185-2196.

RA REPRESEN

Philip L

ABSTRA

methoc
present earch ex
use of ct elastic
is the frequency
calcul hat
smoothed gner
coupled sl tly su
radiation mping

INTRO UCTION

itativ
wate nsid
contributio to sc
functions. elated
representa ns. Ti
situations r whic
to incide ound.
domain onse th
shapes (low sph
reflectin ltrasonic

DISTINC ON BE

F re 1 illu
the phas elocity
surroun g water
arcsin ( ) relative
discussi below).
allow f sonic
couplin rough
radius e shel
considere ould n
such wave for plat
introduce y curv

[1] Present ddress: S
[2] Present ddress: F